

Simulation of current density distribution at PEMFC by using measured electrochemical and physical properties of membrane

Takuto ARAKI, Takuya TANIUCHI and Kazuo ONDA

Department of Electrical and Electronic Engineering,

Toyohashi University of Technology

1-1 Hibarigaoka, Tempaku, Toyohashi, Aichi 441-8580, Japan

Abstract In order to grasp properly PEMFC power generation performances, it is necessary to know factors for water management such as transmissivity and electro-osmotic coefficient of water vapor through the membrane, and factors for power loss such as active and resistive overpotentials. In this study we have measured these factors to analyze our experimental results of PEMFC power generation tests by our two-dimensional simulation code. It considers simultaneously the mass, charge and energy conservation equations, and the equivalent electric-circuit for PEMFC to give numerical distributions of hydrogen/oxygen concentrations, current density, and gas/cell-component temperatures. The numerical distributions of current density under various operating conditions agreed well with the measured distributions by segmented electrodes, which had grooves for hydrogen/oxygen supply and were mold in our test cell being electrically insulated. Hydrogen/oxygen concentration changes measured by gas chromatography along the gas supply grooves gave also the experimental current distributions, which coincided almost with those by the segmented electrodes. Factors to correct the small difference between the measured and the calculated are also discussed from the stand point of the physical meaning of the calculated results considering factors which are not taken into account in our code.

Keywords: Polymer Electrolyte Fuel Cell, Current density distribution, Membrane properties measurement, Numerical model of PEMFC

1. INTRODUCTION

Establishing precise numerical model of the proton exchange membrane fuel cell (PEMFC) provides a useful method to estimate and improve the PEMFC performance. The first objective of the present investigation is to build a numerical model, which can describe the PEMFC performance such as a V-i characteristics and current distributions inside the cell. For building properly the PEMFC model, it is necessary to know the water management factors such as transmissivity and electro-osmotic coefficient of water vapor through the membrane-electrode assembly (MEA), and power loss factors such as activation and resistive overpotentials, since these factors have significant impacts on performance of PEMFC. Nevertheless, the effects by these factors on PEMFC have not been cleared sufficiently. Then, obtaining the basic information for PEMFC is a second objective of this study. The comparison of measured and calculated current distributions is finally conducted to verify the reliability of our numerical model. This comparison between power generating experiments and numerical simulations on a same cell configuration has rarely been reported before. The numerical distributions of current density under various operating conditions agreed well with the measured distributions by segmented electrodes, which had grooves for hydrogen/oxygen supply and were mold in our test cell being electrically insulated. Hydrogen/oxygen concentration changes measured by gas chromatography along the gas supply grooves gave also the experimental current distributions, which coincided almost with those by the segmented electrodes. Factors to correct the small difference between the measured and the calculated are also discussed from the standpoint of the physical

meaning of the calculated results considering factors, which are not taken into account in our code.

2. MEASUREMENTS OF MEMBRANE PROPERTIES AND OVERPOTENTIALS

2.1 Over view of experimental apparatus

An overview of the experimental apparatus is illustrated in Fig. 1 and is basically same as our previous paper^[1]. Fuel (Hydrogen or modified reformed fuel) and oxidant (Oxygen or Air) from gas cylinders are regulated by mass flow controllers, and led to fuel cell (FC). The humidifiers placed before FC control the dew-point temperatures of air and fuel. Electronic resistive load (PLZ-152WA, Kikusui Elec. Co.) is connected to FC instead of actual loading, and measuring the current and voltage of FC. The MEA is set between the two electrodes and carbon cloths are inserted between the MEA and separators as diffusion electrodes. One side of which consist of segmented electrodes with grooves for air or fuel supply and the segmented

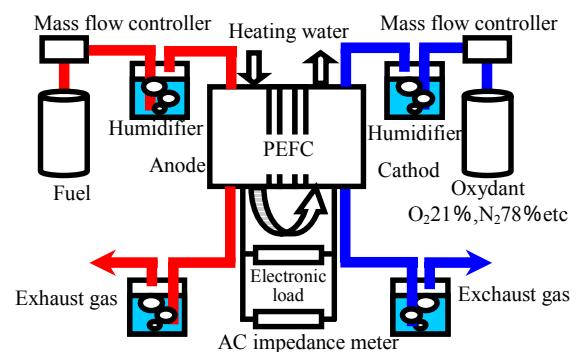


Figure 1 Experimental apparatus

electrodes are mold in an electrically insulating plate for measuring current density distributions. Further information of the experimental conditions will be explained in each section.

2.2 Water Vapor Diffusivity through Diffusion Electrodes, and Transmissivity and Electro-osmotic coefficient through MEA

To obtain the diffusive properties, the cell outlet averaged humidities at both anode and cathode were measured with supplying different humidities to both FC inlets. The pattern diagram of this water (vapor) transport model is depicted in Fig. 2. The mass transfer coefficient at flow velocity v , $h(v)$, increased as gas velocity v increasing, and the diffusive resistance $Rh(v)=1/h(v)\cdot A$ was relatively much smaller than R_{DIF} and R_{MEA} , so that the effect of the mass transfer can be ignored in our experimental conditions.

Measured water vapor diffusivity for diffusion electrode D_{DIF} at cell temperature $T_{mem}=50^\circ\text{C}$ and 60°C are plotted in Fig. 3. The diffusivity did not change against relative humidity. This result is consistent with a simple following equation, ($D_{DIF} = f \cdot D_{Air-H_2O}$), where D_{Air-H_2O} is water vapor diffusivity in air, and f is effective porosity of diffusion electrodes. In the case of out carbon cloth, f is calculated to be about 0.25.

Transmissivity through MEA Tr is also shown in Fig. 3. Our measured Tr was about 7 times higher than the ones by Nguyen *et al.*^[2] and lower than ones by Yamada *et al.*^[3]. However, the tendency of Tr , which rose as relative humidity increase, was consistent with those by Nguyen *et al.* So we approximate Tr as to 7 times greater than those of Nguyen *et al.*

The electro-osmotic coefficient n_d is obtained from the equations shown below and the measured D_{DIF} and Tr :

$$M_x' = h_a(v)(C_a - C_{a,DIF})A \quad (1)$$

$$M_x' = D_{DIF}(C_{a,DIF} - C_{a,MEA})A/d_{DIF} \quad (2)$$

$$M_x' = Tr(C_{a,MEA} - C_{c,MEA})A/d_{MEA} + M_{OSM} \quad (3)$$

$$M_x' = D_{DIF}(C_{c,MEA} - C_{c,DIF})A/d_{DIF} - M_e \quad (4)$$

$$M_x' = h_c(v)(C_{c,DIF} - C_c)A - M_e \quad (5)$$

M_e and M_{OSM} are water flow rate by generated water and electro-osmosis. Then the electro-osmotic coefficient n_d is expressed as

$$n_d = \frac{M_{OSM}}{18} \frac{F}{I} \quad (6)$$

F is Faraday constant and I is the current through the cell. Fig. 4 shows the n_d as a function of relative humidity. The electro-osmotic coefficient n_d became large when the humidity

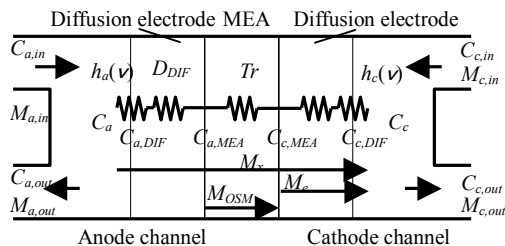


Figure 2 Transport model of water vapor in PEFC

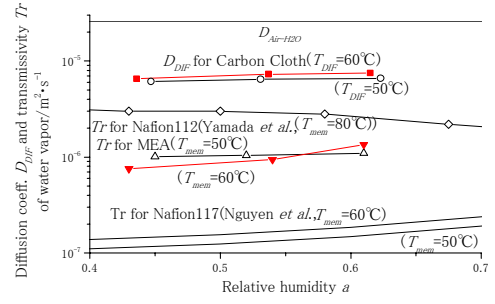


Figure 3 Change of diffusion coefficient D_{DIF} and transmissivity Tr by temperature T_{mem} and relative humidity

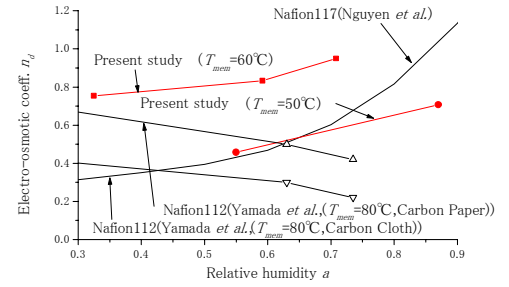


Figure 4 Change of electro-osmotic coefficient by temperature and relative humidity

increases. n_d at MEA temperature of 50°C agreed with that by Nguyen *et al.* n_d by Yamada who performed similar experiment with us was almost same as ours, especially in a case of using carbon cloth, however, the tendency of n_d against humidity was inverse.

2.3 Ionic Resistivity and Activation Overpotential of MEA

Resistive and activative overpotentials are important factors of PEMFC power generation performance. The ionic resistance was measured by AC impedance meter (SOLARTRON SI1280B), supplying air with the same humidity to both anode and cathode to avoid the movement of water through MEA. The parameters for MEA resistance are the membrane temperature T_{mem} and the flow relative humidity a . The resistivity did not depend on the membrane temperature, but depended only on relative humidity a . Therefore the following experimental ionic resistivity ρ , a function of only relative humidity a , was employed in the following numerical analysis.

$$\rho = 57.3 + 383 \cdot \exp\left(-\frac{a-0.089}{0.049}\right) + 244 \exp\left(-\frac{a-0.089}{0.268}\right) \quad (7)$$

For measuring activation overpotential η_{act} , the relatively high flow rates of 600cc/min were provided to hold the low utilization rate of H_2 and O_2 in order to prevent variation of η_{act} along the flow by the distributed current density. η_{act} was derived by subtracting the cell voltage V_{cell} and the resistive overpotential ir from the Nernst potential V_{Nernst} as follows.

$$\eta_{act} = V_{Nernst} - V_{cell} - ir \quad (8)$$

Here, the spatially averaged partial pressures of active materials were used to determine V_{Nernst} considering water vapor pressures. The experimental conditions for η_{act} measurement were as

follows; FC temperature : 60°C, cathode O₂ partial pressure P_{O_2} : 0.05, 0.2, 1.0; anode H₂ partial pressure P_{H_2} : 1.0. Since the activation overpotential increased logarithmically, we adopted following Tafel approximation to compose a empirical formula. The eq.(9) are adopted in following numerical analysis.

$$\eta = A + B \ln i \quad (9)$$

here $A = (-5.15 \times 10^{-4} T + 9.527 \times 10^{-2}) \ln P_{O_2} + 0.433$
 $B = (-1.44 \times 10^{-4} T + 3.584 \times 10^{-2}) \ln P_{O_2} + 0.0234$

3. MEASUREMENT OF CURRENT DISTRIBUTIONS

Current distributions were measured by two different methods to confirm the reliability of measurements. First method adopted the segmented electrodes cell to measure the current distribution by shunt resistances. Another method adopted gas chromatography to measure gas composition changes to be converted to the current distribution through the decreased flow rate of H₂ or O₂. N₂ mixture fuel and air were employed in this measurement to keep the constant flow rate of N₂ as reference. H₂ gas mixed with 20% N₂ (not CO₂) was used as fuel, because CO₂ is easy to be solved in water and not giving the correct reference. The cell configuration of current distribution measurement is illustrated in Fig. 5.

4. NUMERICAL MODEL OF PEMFC

4.1 Numerical procedure

Our model basically consists of the steady state two-dimensional mass, charge and energy conservation equations with an equivalent electric circuit of PEMFC. Following assumptions are adapted to derive governing equations^[2].

1. Fuel cell is a parallel flow type.
2. Gas flow along a channel is plug flow.
3. Owing to the constant-temperature water circulation through separators, the separator temperature is constant. However, temperature changes at PEM and Diffusion layer are considered.
4. The volume of the condensed water is so small that effect by condensed water at cathode can be neglected.
5. The total gas pressure is constant, neglecting pressure drop along flow channel.

The mass conservation equations are as follows by using mole

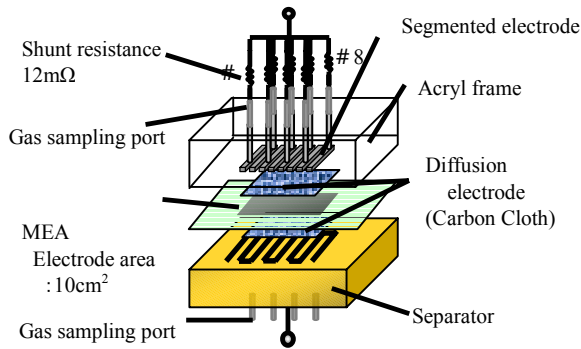


Figure 5 Configuration of cell and segmented electrodes

flow rate M_j of each chemical species j , and current density i through MEA. The subscripts a , c and k denote at anode, cathode and either anode or cathode, respectively. d is height (thickness) of channel (layer) and h is channel width.

$$\text{Hydrogen : } \frac{dM_{H_2}}{dx} = -\frac{hi}{2F} \quad (10)$$

$$\text{Oxygen : } \frac{dM_{O_2}}{dx} = -\frac{hi}{4F} \quad (11)$$

$$\text{Water liquid : } \frac{dM_{water,k}^{liquid}}{dx} = \left(\frac{hd_{channel}}{R(T_k + 273.15)} \right) \left(\frac{M_{water,k}^{vapor}}{M_{water,k}^{vapor} + M_{H_2}} P - P_{water,k}^{saturated} \right) \quad (12)$$

$$\text{Water vapor (anode): } \frac{dM_{water,a}^{vapor}}{dx} = -\frac{dM_{water,a}^{liquid}}{dx} - \frac{dM_{vapor}}{dx} \quad (13)$$

$$\text{(cathode): } \frac{dM_{water,c}^{vapor}}{dx} = -\frac{dM_{water,c}^{liquid}}{dx} + \frac{dM_{vapor}}{dx} + \frac{hi}{2F} \quad (14)$$

Here M_{vapor} is the water vapor mole flow rate from anode to cathode.

$$\frac{dM_{vapor}}{dx} = \frac{R_{MEA} \left(-T_r \frac{dC_w}{dy} + n_d \frac{i}{F} \right) - R_{DIF,c} \frac{i}{2F}}{R_{MEA} + R_{DIF,a} + R_{DIF,c}} h \quad (15)$$

Five energy conservation different equations for five layers (two gas channels, two diffusion electrodes and one MEA) are derived.

The equivalent electric circuit for PEMFC is shown in Fig. 6. Due to the high electric conductivity of the separators, the cell voltage along channel can be kept constant. Control volume method and Tri-diagonal matrix algorithm (TDMA) were used to solve simultaneously equations with an equivalent circuit.

4.2 Comparison of the current distributions with the measured

A current density distributions calculated by the numerical model are shown in Fig. 7 as an example. The conditions for the analysis and experiments are summarized in Table 1. Cathode flow was not humidified to observe the change of current density clearly. Distributions of current densities were increased from inlet as the membrane water content increases by generated water. Then, they decreased from around a middle of a flow channel, since oxygen partial pressure decreased and activation overpotential η_{act} increased along the channel. The position of current peak was shifted downstream as averaged current decreasing, because lower averaged current density i_m means lower water generation speed and lower oxygen consumption

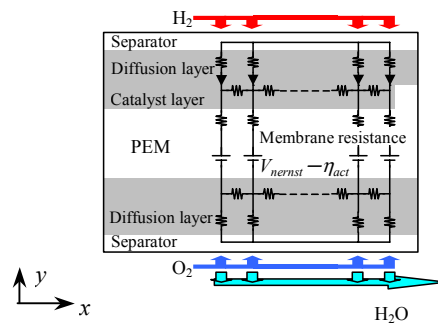


Figure 6 Equivalent electric circuit for the PEMFC

Table 1 Experimental conditions

Cell temperature[°C]	60
Anode flow rate[cc/min]	48
athode flow rate[cc/min]	91
Anode dew temperature[°C]	60
Cathode dew temperature[°C]	Not humidified
Fuel and oxygen utilization ratio($i_m=0.2$ [A/cm ²])	0.4
Fuel and oxygen utilization ratio($i_m=0.3$ [A/cm ²])	0.6
Fuel and oxygen utilization ratio($i_m=0.4$ [A/cm ²])	0.6

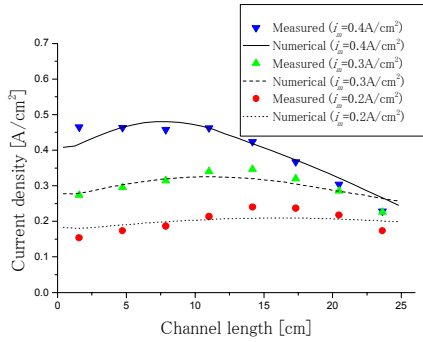


Figure 7 Comparison between the measured and the numerical current distributions (Air flow rate : 91cc/min)

which leads to smaller activation overpotential η_{act} .

The good agreement between the numerical and measured results indicates that our numerical model using the measured water management and power loss factors can provide a useful tool to estimate the PEMFC power generation performance. The measured showed higher current density at inlet, and lower current density at outlet than the calculated, especially for higher oxygen utilization ratio of 80%. This discrepancy might be due to the flooding by generated water at a downstream cathode, hindering the site for electrochemical reaction. Further studies are needed on empirical formula for the activation overpotential, water management factors and diffusion overpotential through diffusion electrode.

1. CONCLUSION

The water management factors such as transmissivity and electro-osmotic coefficient of water vapor through the membrane electrode assembly, and power loss factors such as activative and resistive overpotentials have been measured. These factors were adopted to analyze our experimental results of PEMFC power generation tests by our two-dimensional simulation code. The code considers simultaneously the mass, charge and energy conservation equations with the equivalent electric-circuit for PEMFC to give numerical distribution of hydrogen/oxygen concentrations, current density, and gas/cell-component temperatures along gas flow. The calculated distributions of current density under various operating conditions have agreed well with the measured distributions at

segmented-electrodes cell. Hydrogen /Oxygen concentration changes measured by gas chromatography along the gas flows have also given the experimental current distributions, which coincides almost with that by the segmented-electrodes. Degradation factors for cell performance were also discussed from the numerical results by the simulation code. Also further improvements for our experiment and analysis have been pointed out.

ACKNOWLEDGEMENTS

The present study was conducted in part with the assistance of Chubu Gas Co., LTD. and New Energy and Industrial Technology Development Organization (NEDO).

NOMENCLATURE

A	: membrane active area	[cm ²]
a	: relative humidity	[-]
C	: gas concentration	[g cm ⁻³]
D_i	: diffusion coefficient of species i	[m ² s ⁻¹]
d_l	: thickness of layer l	[cm]
E°	: standard electromotive force	[V]
f	: effective porosity of diffusion electrode	[-]
$h(v)$: mass transfer coefficient at flow velocity v	[cm s ⁻¹]
i_m	: averaged current density	[A cm ⁻²]
i	: local current density	[A/cm ²]
M_x, M_x'	: vapor flow rate	[g s ⁻¹]
M_e	: vapor flow rate of generated water	[g s ⁻¹]
M_{OSM}	: vapor flow rate of electro-osmosis	[g s ⁻¹]
n_d	: electro-osmotic coefficient	[-]
P_i	: partial pressure of gas species i	[atm]
R_l	: gas diffusive resistance of a layer l	
ρ	: membrane resistance	[cm ²]
T_{mem}	: temperature of MEA	[K]
Tr	: transmissivity of MEA	[cm ² s ⁻¹]
V_{cell}	: cell voltage	[V]
V_{Nernst}	: Nernst potential	[V]
v	: supplied gas velocity	[m s ⁻¹]
w_{cell}	: cell width (channel width + rib width)	[cm]
η_{act}	: activation overpotential	[V]
η_{ohm}	: resistive overpotential	[V]
ρ	: membrane resistivity	[cm]

(Subscripts)

a, c	: anode and cathode
liq, vap	: liquid and vapor
mem	: membrane
DIF	: diffusion electrode

REFERENCE

- [1] T.Kyakuno, K.Hattori, K.Ito and K. Onda, Proc. 2003 IEEE Conf., (2003) 7-151. (in Japanese)
- [2] T.V.Nguyen and R.E.White, J. Electrochem. Soc., Vol.140, No8, (1993) p.2178.
- [3] H.Yamada and Y.Morimoto, Proc. 70th anniversary Jpn. Electrochem., Soc. (2003) p316. (in Japanese)
- [4] T. Aoki, N. Miyauchi, K. Ito, Y. Inui and K. Onda: Numerical Analysis of Polymer Electrolyte Fuel Cell Using Empirical Equations for Overpotentials. Trans. IEE Japan, Vol. 122-B, No. 12, (2002). (in Japanese)
- [5] S. V. Patankar, Numerical Heat Transfer and Fluid Flow, Hemisphere Publishing, pp.24-56 (1985).